Synthetic and Systems Biotechnology 7 (2022) 765–774

Contents lists available at ScienceDirect

Synthetic and Systems Biotechnology

journal homepage: www.keaipublishing.com/en/journals/synthetic-and-systems-biotechnology

Original Research Article

Development of a novel platform for recombinant protein production in *Corynebacterium glutamicum* on ethanol

Xinyu Yu [a,b,d], Xiuxia Liu [a,b,d,*], Xiong Gao [c], Xunxun Luo [e,f], Yankun Yang [a,b,d], Ye Li [a,b,d], Chunli Liu [a,b,d], Chong Zhang [e,f], Zhonghu Bai [a,b,d]

[a] Key Laboratory of Industrial Biotechnology, Ministry of Education, School of Biotechnology, Jiangnan University, Wuxi, China
[b] National Engineering Research Center for Cereal Fermentation and Food Biomanufacturing, Jiangnan University, Wuxi, China
[c] Division of Life Science, The Hong Kong University of Science and Technology, Clear Water Bay, Hong Kong, China
[d] Jiangsu Provincial Research Center for Bioactive Product Processing Technology, Jiangnan University, Wuxi, China
[e] MOE Key Laboratory for Industrial Biocatalysis, Institute of Biochemical Engineering, Department of Chemical Engineering, Tsinghua University, Beijing, China
[f] Center for Synthetic and Systems Biology, Tsinghua University, Beijing, China

ARTICLE INFO

Keywords:
Corynebacterium glutamicum
Ethanol
Transcriptional engineering
Secretory protein overexpression
NEO-2/15

ABSTRACT

Corynebacterium glutamicum represents an emerging recombinant protein expression factory due to its ideal features for protein secretion, but its applicability is harmed by the lack of an autoinduction system with tight regulation and high yield. Here, we propose a new recombinant protein manufacturing platform that leverages ethanol as both a delayed carbon source and an inducer. First, we reanalysed the native inducible promoter P_{ICL} from the acetate uptake operon and found that its limited capacity is the result of the inadequate translation initial architecture. The two strategies of bicistronic design and ribozyme-based insulator can ensure the high activity of this promoter. Next, through transcriptional engineering that alters transcription factor binding sites (TFBSs) and the first transcribed sequence, the truncated promoter P_{A256} with a dramatically higher transcription level was generated. When producing the superfolder green fluorescent protein (sfGFP) under 1% ethanol conditions, P_{A256} exhibited substantially lower protein accumulation in prophase but an approximately 2.5-fold greater final yield than the strong promoter P_{H36}. This superior expression mode was further validated using two secreted proteins, camelid antibody fragment (VHH) and endoxylanase (XynA). Furthermore, utilizing CRISPRi technology, ethanol utilization blocking strains were created, and P_{A256} was shown to be impaired in the phosphotransacetylase (PTA) knockdown strains, indicating that ethanol metabolism into the tricarboxylic acid cycle is required for P_{A256} upregulation. Finally, this platform was applied to produce the "de novo design" protein NEO-2/15, and by introducing the N-propeptide of CspB, NEO-2/15 was effectively secreted with the accumulation 281 mg/L obtained after 24 h of shake-flask fermentation. To the best of our knowledge, this is the first report of NEO-2/15 secretory overexpression.

1. Introduction

The expansion of biologics and the biopharmaceutical industry has fuelled the demand for recombinant proteins in recent years [1,2]. As the major factor influencing product quality and process cost, the selection of biological platforms used as cell factories is particularly important [3,4]. For structurally simple proteins that do not require posttranslational modifications, prokaryotic cells, particularly *Escherichia coli*, are still the preferred expression systems [5]. However, considering that secreting the desired protein into the supernatant significantly simplifies downstream processing and reduces the total cost [6,7], several gram-positive bacterial expression systems with prominent secretory capacity have recently been developed [8,9]. Among them, *Corynebacterium glutamicum*, the long-established industrial workhorse for the production of a variety of amino acids [10], possesses enormous potential for the secretory production of recombinant proteins due to its safety, excellent fermentation performance and concise secretory environment (minimal endogenous secretory proteins and rarely detectable protease activity) [11].

For a high-performance expression system, optimal promoter

Peer review under responsibility of KeAi Communications Co., Ltd.
* Corresponding author. School of Biotechnology, Jiangnan University, Wuxi, 214122, China.
E-mail address: liuxiuxia@jiangnan.edu.cn (X. Liu).

https://doi.org/10.1016/j.synbio.2022.03.004
Received 21 November 2021; Received in revised form 4 March 2022; Accepted 15 March 2022

sequences and efficient regulatory mechanisms are essential prerequisites; thus, many attempts have been made to enhance protein yield through promoter engineering. The methods for obtaining promoters with desirable properties and strength in *C. glutamicum* fall into three main categories: 1) mutagenesis of the existing strong promoters, e.g., the tac-M promoter with an extended −10 region mutation [12]; 2) a fully synthetic library, e.g., the H36 promoter from a 70-bp random sequence library [13]; 3) screening naturally occurring promoters (NOPs) [14]. Several regulatable NOPs have been identified by screening under specific conditions, e.g., maltose and gluconate-inducible promoters [15], which are beneficial for protein production without impacting cell proliferation. Moreover, there is usually an extended regulatory region upstream of NOPs, which contains multiple TFBSs, and transcriptional engineering through modification of TFBSs has been demonstrated to be an effective strategy to optimize promoter strength and regulation in eukaryotic cells [16,17].

The *AOX1* promoter of *Pichia pastoris* is the typifier of NOP, which was identified from the methanol utilization pathway and widely used for protein production with extraordinary strength and tight regulation [18]. Inspired by this, we noted the possibility of ethanol as a supplementary carbon source and inducer for protein production in *C. glutamicum*. First, ethanol as a carbon source is consistent with the biorefinery concept due to its unlimited availability and environmental friendliness. Second, *C. glutamicum* is able to use ethanol as the sole carbon source with an appreciable biomass yield [19]. Third, the utilization of ethanol in *C. glutamicum* has a delayed effect. Biphasic growth behaviour could be observed on mixed carbon source medium, which was caused by the sequential utilization of glucose before ethanol [19]. Finally, unlike the "permeability repression" of inducers such as isopropyl-b-D-thiogalactopyranoside (IPTG) and L-arabinose [20], ethanol, as an amphipathic molecule, is freely permeable across bacterial membranes.

In this work, we reanalysed the promoter of isocitrate lyase (ICL), the key enzyme triggering the ethanol utilization (EUT) pathway of *C. glutamicum*, and demonstrated its capability as a powerful NOP when a conservative translation initiation structure is intact. Through transcriptional engineering based on TFBSs and UTR (Untranslated Region) modification, we generated an enhanced ethanol-activated promoter P_{A256}, which maintains low activity in early growth but exhibits extraordinary strength during the ethanol utilization phase. By comparing the activity of P_{A256} in various EUT-blocking strains, we found that the activation of acetyl-CoA by acetyl phosphate is the key premise for the upregulation of P_{A256} on ethanol. Finally, efficient protein production with P_{A256} over the EUT pathway was successfully demonstrated with three recombinant proteins: VHH, XynA and NEO-2/15.

2. Materials and methods

2.1. Bacterial strains and growth conditions

E. coli DH5α was used as a cloning host for plasmid construction and cultivated in Luria–Bertani (LB) medium (per litre 1% tryptone, 0.5% yeast extract and 1% NaCl), which was supplemented with 30 μg/mL chloramphenicol or 50 μg/mL kanamycin when necessary. *C. glutamicum* CGMCC 1.15647 (GenBank: CP073911.1) was used for the construction and analysis of expression systems and cultivated at 30 °C in LBB medium (LB supplemented with 1% brain heart infusion, 10 μg/mL chloramphenicol and 25 μg/mL kanamycin when necessary). Shake-flask fermentation (10 mL medium in each 100-mL shake flask) and 24-deep-well plate fermentation (1 mL medium in each 5-mL hole) were carried out to assess the protein expression of different constructs. Absolute ethanol was added directly to the LBB medium by volume ratio when needed. Noncolony-type monolayer culture (NCM) medium supplemented with cell wall weakening agents was used to make competent cells [21]. LBHis medium (5 g/L tryptone, 2.5 g/L yeast extract, 18.5 g/L brain heart infusion broth, 91 g/L sorbitol and 5 g/L NaCl) was used for transformation of *C. glutamicum*.

2.2. Protein extraction and analysis

For intracellular protein analysis, the culture of *C. glutamicum* (adjusted to 1 mL, OD_{600}~10.0) was harvested by centrifugation and washed twice with PBS, then resuspended in 1 mL PBS. Cell lysis was carried out using Ultrasonic breaker Vibra cell VCX500 (SONICS) and lysis supernatant after centrifugation was used for SDS-PAGE analysis. For extracellular protein analysis, after centrifugation, the medium supernatant was collected and directly subjected to denaturation (25 μl supernatant+5 μl protein loading buffer, 98 °C, 8min), with 15 μl denaturated sample loaded on each lane for SDS-PAGE analysis.

The protein band of interest in the ethanol-induced sample was extracted as granules (1 mm), which were then destained in decolorizing buffer and lyophilized at 4 °C. The lyophilized sample was immersed in porcine trypsin solution and incubated within NH_4HCO_3 buffer at 37 °C for 12 h. MALDI-TOF-MS was applied to analyse digested fractions from the SwissProt database to identify the target protein.

Western blotting assays were performed to confirm NEO-2/15 (6 × histidine tag at the C-terminal) expression and secretion in *C. glutamicum*. The proteins of the identical SDS–PAGE gel were electrophoretically transferred onto a Polyvenylidenfluoride (PVDF) membrane. The membrane was washed with TBST and incubated in blocking buffer (TBST containing 5% nonfat milk powder) for 2 h. Then, the PVDF membrane was incubated in antibody solution (monoclonal horseradish peroxidase-conjugated anti-His6 antibody) for 1 h and washed three times with TBST. Finally, the binding of the antibody was detected using an ECL kit and imaging system.

2.3. Promoter reporter vectors and protein expression vectors

The main strains and plasmids used in the study are listed in Table S1. The important primers and oligonucleotides are listed in Table S2. Taq or KOD-plus-neo polymerases (Toyobo) were used for PCR. The shuttle vector p19-0 [22] was the backbone for all expression vector construction. Genomic DNA of *C. glutamicum* and *Corynebacterium ammoniagenes* ATCC 6872 were extracted using a TIANamp Bacteria DNA Kit and used as a template to amplify the promoter fragment. For enhanced green fluorescent protein (eGFP) expression, the promoter fragment and eGFP fragment (additional SD sequence if necessary) were integrated into p19-0 by Gibson assembly [23]. For sfGFP expression, the plasmid p19-RiboJ-sfGFP containing the spacer, RiboJ, RBS and sfGFP sequences was constructed, and the *Xho*I restriction site between spacer and RiboJ was used for the insertion of promoter variants by Gibson assembly. To generate VHH- and XynA-expressing plasmids, the codon-optimized *vhh* (GenBank: MZ622246) and *xynA* (GenBank: MZ622248) for *C. glutamicum* were PCR-amplified with a C-terminal tetracysteine tag and cloned into the p19-0 vector with the promoter-RiboJ-RBS fragment and signal peptide fragment. To generate NEO-2/15-expressing plasmids, the P_{A256}-RiboJ-RBS fragment and codon-optimized *neo* fragment (6His-tag$^+$, GenBank: MZ545408) were integrated into the p19-0 vector with various N-terminal peptide fragments. All plasmids were confirmed by Sanger sequencing and introduced by electroporation into competent *C. glutamicum* cells according to protocols described previously [21].

2.4. Quantification of protein expression levels

To quantify the expression levels of eGFP/sfGFP in *C. glutamicum*, cells cultured for 24/36 h were harvested, washed and resuspended. Cell suspensions were diluted to remain within the linear range of the plate reader (1:40-fold, i.e., Fifty microlitres of cell suspension was added to 1950 μl of ddH_2O, 200 μl for fluorometry and 1000 μl for OD measurement. The fluorescence intensity of each sample was measured using

a multimode plate reader (Tecan Infinite Pro 200, Switzerland) and normalized by the cell optical density OD600 to correct for dilution errors and different amounts of cell material.

To quantify the expression levels of secreted VHH/XynA, the supernatant of each culture was diluted to remain within the detection line of 1 μM FlAsH-EDT_2 (VHH 1:10-fold, XynA 1:4-fold). A total of 180 μl of the diluted sample was mixed with 20 μL of concentrated assay cocktail (10 μM FlAsH-EDT_2, 10 mM DTT) following incubation for 1 h, and the fluorescence was measured by 485 nm excitation and 528 nm emission. To quantify the production of secreted NEO-2/15, the total protein concentration of the fermentation supernatant was measured using the Detergent Compatible Bradford Protein Quantification Kit (Vazyme). A standard calibration curve was plot using eight concentrations of Bovine Serum Albumin: 100 μg/mL, 200 μg/mL, 400 μg/mL, 800 μg/mL, 1000 μg/mL. Culture supernatant of strains harbouring the empty vector was used as background to calculate the secretion yield of the target protein.

2.5. Construction and validation of the all-in-one CRISPRi system

To construct a single plasmid CRISPRi system, the codon-optimized *dCas9* gene (GenBank: MZ622250), terminator and sgRNA expression cassette were chemically synthesized as one fragment and cloned into the pEC-XK99E vector. The sgRNA expression cassette contained a Ptrc sequence without the 5′UTR, a 20 bp sgRNA coding sequence, and a sgRNA scaffold (dCas9 handle and *S. pyogenes* terminator) sequence. Two *Bsa*I restriction sites separated by spacers (as exemplarily shown in Fig. S5) allowed easy insertion of sgRNA fragments using the Golden Gate method [24]. For sgRNA design, N20NGG motifs were searched in the template strand of the target gene, and those located within the first 150 bp of the open reading frame (ORF) were selected as candidates. Off-target effects were checked in the *C. glutamicum* CGMCC 1.15647 genome using the SeqMap package [25]. Candidates with a tolerance setting of five mismatches and 40–60% GC content were used for interference experiments, which were obtained by annealing two oligonucleotide chains. Nontargeting sgRNAs were designed by random generation of N20NGG with the proper GC content, and those with more than two mismatches within 12 bp of the PAM region were selected.

To repress the expression of the *egfp* gene, a sgRNA targeting+32 position of the ORF was designed, and the corresponding CRISPRi plasmid was transformed into P_{ICL}-B constructs. The blank vector without sgRNA was also transformed as a negative control. Fluorescence was characterized as mentioned above, and intracellular expression of eGFP was observed through fluorescence microscopy. We further tested the reliability of our system by targeting the CRISPRi machinery to *porB, pgi, and pyk* (three genes had been knocked down or knocked out in other work and had no effect on growth), and three sgRNAs per gene targeting at different positions were tested. The transcriptional levels of targeted genes were quantified by quantitative reverse transcription PCR (qRT–PCR), total RNA purification and qRT–PCR analysis were performed as described previously [26], and the $2^{-\Delta\Delta Ct}$ method was adopted with *gyrb* (NCgl2772) as the housekeeping gene. The level of each gene in the wild-type strain was defined as 1.0.

2.6. CRISPRi-based regulation of genes involved in the EUT pathway

To block the EUT pathway, the genes *adh* (NCgl2382), *aldh* (NCgl2698), *ak* (NCgl2657), *pta* (NCgl2656), *aceA* (NCgl2248), and *aceB* (NCgl2247), which are encoding enzymes involved in the EUT pathway, were selected as individual targets for repression by our CRISPRi system. The sgRNAs were designed according to the above, annealing onto the first 150 bp of the NT strand of each gene. The CRISPRi plasmid containing the desired sgRNA was transformed into strains expressing sfGFP driven by P_{A256}, and three nontargeting sgRNAs were used as controls. For the induction of CRISPRi, 1 mM IPTG was added to the medium.

2.7. Statistical analysis

Values and error bars reflect the mean ± s.d. of three biological replicates (n = 3). All P values were generated from two-tailed t-tests using the Microsoft Excel 2016 (Microsoft Corporation, USA).

3. Results

3.1. Identification and utilization of the representative NOP on ethanol

Comprehensive mRNA analysis of transcriptomics and a full range of proteins detected using proteomics are feasible approaches for screening NOPs with high strength for optimized gene expression [27]. To identify the representative ethanol-regulated NOP in *C. glutamicum*, an extra 1% (v/v) ethanol was added to the complex medium LBB, and an unknown protein with a molecular weight of ~45 kDa was observed to accumulate considerably in the cytoplasm (Fig. 1a). The corresponding band was extracted, and MALDI-TOF-MS analysis showed that the protein is isocitrate lyase (ICL, GenBank: BAB99724.1), which is the key enzyme of the glyoxylate cycle [28]. The CRISPRi technique (see Section 3.4) was used to construct the gene knockdown mutant and verify this result. A nontemplate-strand targeting sgRNA was designed to block transcription of the isocitrate lyase gene *aceA*, while a nontargeting sgRNA served as a control. The results showed that in knockdown mutants cultivated in ethanol, the corresponding band was missing (Fig. 1a, Lane 4). Meanwhile, knockdown mutants exhibited a defect in ethanol utilization (Fig. 1b), which is consistent with a previous report [19] that ICL is required for the growth of *C. glutamicum* on ethanol. These results suggested that *aceA* exhibits the most visible changes in protein abundance upon shifting to ethanol as a carbon source; thus, we refocused our attention on its native promoter P_{ICL}. The gene *aceA* and the malate synthase gene *aceB* are transcribed in opposing directions, forming a single operon [29], and the mRNA levels of *aceA* and *aceB* were 6-fold and 7-fold higher, respectively, in ethanol-grown cells than in glucose-grown cells [19]. However, in the updated study [30], RNase E/G breakage was detected in the 3′UTR of mature *aceA* RNA (approximately 3-fold higher mRNA level and 4 times longer half-life of the *aceA* gene in *rneG* knockout mutants), indicating that the practical activity of P_{ICL} is greater. Given that the endogenous 3′UTR is not employed in the expression of foreign genes, we speculated that P_{ICL} would be an appropriate choice for building the recombinant protein manufacturing platform.

Using eGFP as a reporter, we evaluated P_{ICL} activity under three different strategies. First, the 483 bp *cis*-regulatory region (called P_{ICL}-M) upstream of the start codon ATG was intercepted and directly followed by the *egfp* gene; however, only a few fluorescent signals were detected. The RBS Calculator (predict mode, version: v2.1.1) [31] indicated that the translation initiation rate of this architecture was extremely low (only 2.06, au). Hence, P_{ICL}-U was constructed by replacing the endogenous 5′UTR with the 5′UTR from monocistronic Ptac [32] to ensure effective translation initiation. Furthermore, the bicistronic design (BCD) expression cassette, a ‘context preservation’ strategy often employed to repair NOPs [33,34], was used to preserve the original translation initiation structure and improve expression via the translational coupling effect [35]. For this, 62 bp from the N-terminal coding region of ICL and additional SD2 were inserted as fore-cistrons (encoding a 25-amino-acid peptide), and the resulting bicistronic promoter was designated P_{ICL}-B (Fig. 1c). Given the increased biomass from ethanol utilization, the relative fluorescence unit (rfu) of each construct was divided by the corresponding OD_{600} to normalize the expression of fluorescent protein. As the results showed (Fig. 1d), when grown with 1% ethanol added, both P_{ICL}-U and P_{ICL}-B constructs showed obvious fluorescence, with the latter being 3.5-fold higher. Meanwhile, in P_{ICL}-B constructs, the eGFP expression level after induction was 10 times higher than that in the uninduced state. Overall, after translational structural adjustment, the NOP of isocitrate lyase displayed significant

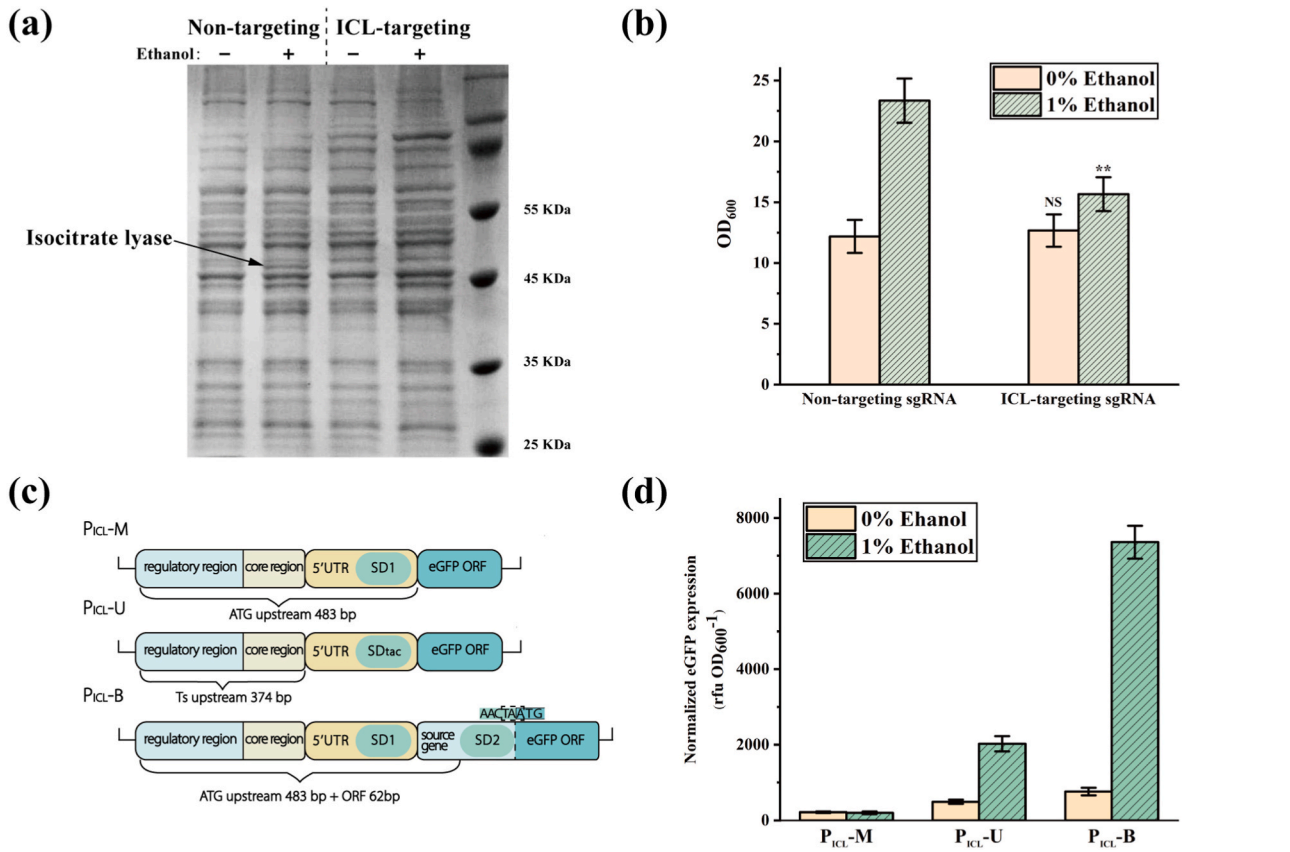

Fig. 1. Characterization of the representative NOP in *C. glutamicum* on ethanol. (a) SDS–PAGE analysis of total intracellular proteins from the control strain harbouring dCas9 and nontargeting sgRNA and the ICL knockdown strain harbouring dCas9 and ICL-targeting sgRNA. Both cell samples were grown without or with 1% (v/v) ethanol, which are indicated by the symbols – and +. Strains were cultivated in shake flasks for 24 h to obtain enough cells for the analysis of intracellular proteins. (b) Growth of the ICL knockdown strain and the control strain in LBB medium containing 0% or 1% ethanol. Bacterial culture was conducted in shake flasks for 24 h (0% ethanol) and 36 h (1% ethanol). Values and error bars reflect the mean ± s.d. of three biological replicates (n = 3). Statistical differences between the ICL knockdown strain and the control strain were determined by Student's two-tailed test. NS, not statistically significant. $^{**}P < 0.01$, n = 3. (c) Architectures of three strategies using the promoter of ICL to initiate the expression of eGFP. P_{ICL}-M, the intrinsic ORF, was directly replaced with an ORF that encodes eGFP; P_{ICL}-U, the intrinsic 5′UTR, was replaced with the 5′UTR of P_{tac} from the pXMJ19 vector; P_{ICL}-B contained two additional elements to form the BCD expression cassette: the 62bp N-terminal ORF sequence of the source gene and a second SD (Shine-Dalgarno sequence) sequence. (d) Comparison of eGFP expression among the three strategies. The protein expression was conducted in shake flasks for 24 h (0% ethanol) and 36 h (1% ethanol). Data are presented as the mean values ± s.d. of three biological replicates (n = 3).

activity for heterologous protein overexpression and tight regulation by ethanol.

3.2. Transcriptional engineering of the isocitrate lyase promoter

The transcription start site (TSS) of P_{ICL} has been reported to be located −112 bp upstream of the start codon ATG, where a bidirectional core promoter (separate −35 elements and an overlapping −10 element) and a TG trimer were found nearby [36]. Furthermore, P_{ICL} has been demonstrated to be regulated by the global transcription factors RamA, RamB, and GlxR, similar to the promoters of other central metabolism genes [37]. Six RamA binding sites (Abss) were found in the upstream regulatory sequence of P_{ICL} [38] and a RamB binding site (Bbs) was located between the 4th Abs and the 5th Abs [39]. In addition, a binding site of GlxR (a global TF of the cAMP receptor protein family) [40] closely follows the 3rd Abs (Fig. 2a, Text S1). To investigate the effect of various TFBSs on promoter activity, we created a series of promoters with truncated upstream regulatory sequences of 486 bp, 371 bp, 301 bp, 256 bp, 234 bp, 223 bp, 205 bp, 148 bp, 116 bp, 87 bp, 72 bp, and 59 bp (before the TSS) while keeping the native UTR, which we called P_{ANNN}UTR. Considering the abovementioned negative impact of the native UTR on translation efficiency and to ensure that all modifications act at the transcription level, the insulator RiboJ composed of a hammerhead ribozyme and downstream hairpin [41] was introduced to generate uniform transcripts for sfGFP expression (Fig. 2b). The strength of these truncated variants was compared to the powerful synthetic promoter H36 (P_{H36}, with RiboJ) under ethanol and nonethanol conditions (culture time t = 24 h and t = 36 h, respectively). After induction with 1% ethanol, the specific fluorescence of full-length P_{ICL} (P_{A486}UTR) increased 2.85-fold compared with the uninduced state but was approximately 10% lower than that under the P_{H36} promoter (Fig. 2c). The promoter strength did not change significantly when shortened from 486 to 301 bp, demonstrating that there is no effective *cis*-acting element in this scope. Surprisingly, after removing the 1st Abs (i.e., P_{A256}UTR), the expression level was 3.62-fold greater than before it was eliminated. Despite the fact that sfGFP expression with P_{A256}UTR increased dramatically in the absence of ethanol, identical induction ratios (2.78-fold) were maintained. When the 2nd Abs (P_{A234}UTR) was deleted, the promoter's activity was drastically reduced, and subsequent truncated versions maintained a very low expression level. No additional inducing activity was observed when the Bbss (P_{A87}UTR, P_{A72}UTR) were removed. Overall, we investigated the significance of several TFBSs in P_{ICL} transcription by truncating the upstream regulatory area, finding that the most distant RamA binding motif (1st Abs) to the TSS has a significant inhibitory effect, but the 2nd Abs has a positive effect on transcription. The P_{A256}UTR promoter generated by removing

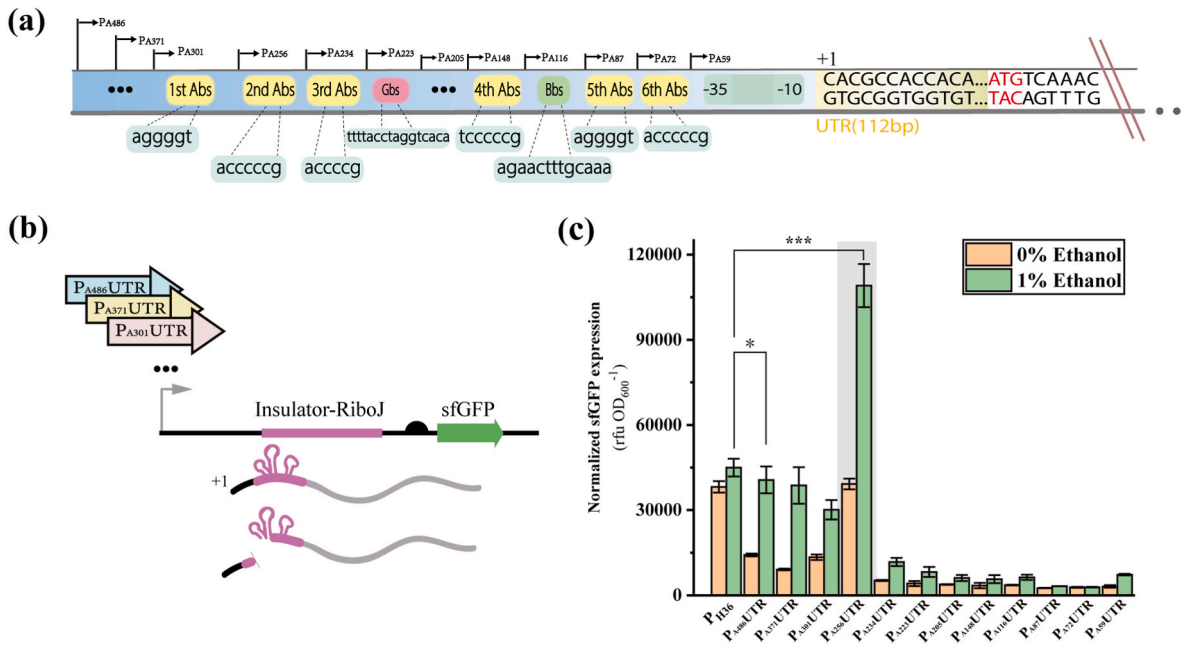

Fig. 2. Transcriptional engineering of the isocitrate lyase promoter. (a) The cis-acting elements characterized in the upstream regulatory sequence of P_{ICL}. The truncated position is indicated by a black arrow. The TSS is denoted as +1, and the native UTR is highlighted in yellow. The start codon is marked in red. (b) Schematic diagram of expressing sfGFP with RiboJ. All truncated promoter and control promoter sequences were inserted upstream of RiboJ. Under any promoters inputting, ribozyme RiboJ cleaves internally, to remove the 5' sequence from the promoter, thus forming the same mRNA for sfGFP translation. (c) The promoter strength of truncated P_{ICL} promoters under ethanol and nonethanol conditions. The sfGFP expression was conducted in shake flasks for 24 h (0% ethanol) and 36 h (1% ethanol). Values and error bars reflect the mean ± s.d. of three biological replicates (n = 3). $^{*}P < 0.05$, $^{***}P < 0.001$, Student's two-tailed *t*-test.

the 1st Abs displayed extraordinarily high sfGFP expression, which was 2.43-fold greater than that achieved with P_{H36} on 1% ethanol.

Another key element determining promoter transcriptional activity is RNA polymerase escape efficiency, which is influenced by both the core promoter and the first transcribed sequence [42]. The core region and the native UTR of P_{A256}UTR were shortened for this purpose to study their impact on transcription. A series of forward and reverse truncated variants surrounding the TSS were generated and evaluated for sfGFP expression. As the results showed (Fig. S1), different degrees of 5′UTR retention resulted in significantly varied transcriptional activity, with P_{A256}U20 exhibiting the highest expression level, approximately 1.45-fold higher than P_{A256}U0 and 2.59-fold higher than P_{H36}. Therefore, retaining the 20 bp endogenous UTR is required to enable the optimum activity of P_{ICL}. Furthermore, removing the entire native UTR, including the −35 element responsible for *aceB* transcription start (P_{A256}U0 constructs), only resulted in a minor decrease in promoter activity compared to P_{A256}UTR, demonstrating that native UTR and bidirectional transcription structure are not essential for P_{ICL}-oriented transcription. The TG dimer near the −10 element, on the other hand, has been reported to significantly increase promoter activity in *C. glutamicum* [43], but our results showed that the TG trimer of P_{ICL} has no significant effect on its transcriptional activity because similar sfGFP expression levels between the P_{A256}U0 and P_{A256}M10 constructs were observed. As expected, the removal of the −10 element prior to the TG trimer (i.e., P_{A256}M20) caused the deactivation of the promoter. We attempted to further minimize the redundant sequence of the regulatory region using internal deletions on the basis of P_{A256}U20. However, eliminating the in-between sequence of Gbs and the 3rd Abs or deleting the internal Abs and Bbs motifs severely impaired promoter activity (Fig. S1). As a result, in all subsequent tests, the P_{A256}U20 structure (hereafter abbreviated as P_{A256}) was employed.

3.3. Expression capabilities and limitations of P_{A256}

To better understand the protein overexpression controlled by P_{A256} on ethanol, the growth and sfGFP expression curves of P_{A256}-sfGFP constructs were examined (Fig. S2a). The results showed that, whether ethanol was given or not, P_{A256}-sfGFP constructs had significantly lower expression levels than those under the P_{H36} promoter in the early growth period (3 h, $P < 0.01$) and on plates (Fig. S3). Furthermore, diauxic growth could be observed with 1% ethanol added, and the sfGFP expression level with P_{A256} dramatically increased in the second stage (after 6 h). Thus, P_{A256} provides a better production mode with both a proliferation phase and a production phase, which is critical for the overexpression of heterologous proteins, particularly toxic proteins. To find the best ethanol concentrations for the induction of P_{A256}, ethanol concentrations ranging from 0.5% to 5% (v/v) were investigated (Fig. S2b). When the ethanol concentration was less than 2.5%, the biomass of P_{A256}-sfGFP constructs rose as the ethanol concentration increased, with the maximum unit expression levels attained on 1–2% ethanol (no significant difference between the 1%, 1.5% and 2% groups). Higher ethanol concentrations (>2.5%) decreased cell metabolism and lowered the growth rate, which is consistent with the optimum ethanol concentration for *C. glutamicum* growth previously discovered by Arndt et al. [19]. Meanwhile, the expression level of P_{A256} was reduced when exposed to more than 2.5% ethanol.

In addition, the promoter strength of P_{A256} was compared to that of other endogenous strong promoters of corynebacteria. Several native promoters of genes, P_{dapA}, P_{tuf} and P_{cspB} from *C. glutamicum* and CJ4 (P_{tuf}), CJ5 (P_{gapA}) and CJ6 (P_{cysK}) from *Corynebacterium ammoniagenes*, were cloned and integrated into the p19-RiboJ-sfGFP vector, and their strengths were tested under ethanol and nonethanol conditions. Among all investigated promoters, only P_{A256} demonstrated a significant induction by ethanol, and the sfGFP expression with P_{A256} was considerably higher than with others (Fig. S4b). Furthermore, we evaluated the activity of these promoters in *E. coli* and observed that only P_{A256}, P_{H36}, P_{dapA} exhibited limited transcription activities in *E. coli*, making them capable of assembling expression vectors for recombinant proteins with high host toxicity (Fig. S4a).

3.4. Activity of P_{A256} in the EUT blocking strains

After passing through the cell membrane, ethanol is oxidized via acetaldehyde to acetate, which then enters the TCA cycle after being activated to acetyl coenzyme A (Fig. 3a). To identify the key steps determining the upregulation of P_{A256}, we attempted to disrupt each step by interfering with key genes in the EUT pathway. We created a single plasmid CRISPRi system (Fig. S5) on the pECXK99E vector (pGA1 replicon) for this purpose, which is compatible with the A256 expression system established on the pBL1 replicon-derived vector. To control dCas9 expression, the $LacI^Q$ repressor system was employed, and the sgRNA expression cassette referred to bacterial CRISPRi system design guidelines [44]. To investigate the efficacy of CRISPRi for gene repression in *C. glutamicum*, four genes were chosen as targets (*egfp* in the P_{ICL}-B construct and the endogenous genes *porB, pgi, and pyk*) and were all effectively knocked down (Fig. S5).

Based on the foregoing results, we established CRISPRi system dependability and used it to block the EUT pathway in P_{A256}-controlled sfGFP-expressing strains. We designed one sgRNA for each of the six key genes involved in the EUT pathway, and three nontargeting sgRNAs were utilized as negative controls (Fig. 3b). Each sgRNA was integrated into the CRISPRi plasmid and cotransformed into wild-type strains with the P_{A256}-sfGFP plasmid. The growth and sfGFP expression of these constructs were evaluated in ethanol and nonethanol environments (Fig. 3c). The results indicated that most knockdown strains grew normally under nonethanol circumstances, with the exception of the ALDH knockdown strains, which had 18.1% less biomass than the control strains. Under ethanol conditions, the knockdown strains exhibited varying degrees of growth impairment (the final biomass was lowered to 44.2–90.6% of the control strains). Among them, the ALDH knockdown strains showed similar growth levels as when no ethanol was given; i.e., the biomass growth due to ethanol addition was reduced from 110.9% to 13.7%, demonstrating that the suppression of ALDH caused the strains to lose their capacity to use ethanol almost entirely. Except for the PTA knockdown strains, the sfGFP expression level regulated by P_{A256} dropped in all knockdown strains but preserved a certain ethanol-induced impact (induction ratios ranging from 1.35 to 2.22). In contrast, P_{A256} activity was substantially hampered in the PTA knockdown strains under ethanol conditions (a loss of 96% of expression relative to the control strains), although it operates effectively when ethanol is not present. It should be noted that the genes encoding AK and PTA (*ack* and *pta*, respectively) form a bicistronic operon, with *pta* upstream of *ack*, suggesting that there might be a forward polar effect, i.e., targeting the CRISPRi complex to the ORF of *pta* is likely to inhibit *ack* transcription. As a consequence, P_{A256} inactivation might be an independent impact of PTA knockdown, or it could be the result of simultaneous suppression of PTA and AK. At the very least, the current data suggest that the elevated activity of P_{A256} is the consequence of ethanol metabolism, particularly when ethanol is metabolized into the TCA cycle.

3.5. High-level production of secretory proteins with P_{A256}

To demonstrate the adaptability of P_{A256} for proteins with a larger range of molecular weights, we applied it to the production of two secretory proteins, VHH (15 kDa) and XynA (47 kDa), both of which have achieved high yield production with the P_{H36} promoter [45]. To monitor and compare the yield of the target protein in the culture supernatant, we applied the FlAsH-tetracysteine system to our experiments. To this end, an optimized biarsenically binding tetracysteine motif (-FLNCCPGCCMEP-) [46,47] was genetically fused to the C-terminus of the target proteins (Texts S2 and S3), which was specifically recognized by the fluorescein derivative with two As(III) substituents, FlAsH-EDT_2 [48], and the fluorescence produced corresponded with the content of labelled proteins (Fig. 4a). The reliability of this approach was demonstrated by inducible P_{tac}-controlled VHH secretory expression (Fig. S6). For the secretory expression of VHH and XynA, the endogenous signal peptide of CspB [49] (spCspB) was used, and several RBSs with different predicted translation initiation rates were tested to ensure translation efficiency with spCspB as the N-terminal sequence (Fig. S7). With the optimal RBS, we constructed spCspB-guided VHH- and XynA-expressing strains with P_{A256} and P_{H36}, and the secretory expression under the control of these two promoters was compared on 1% ethanol. In the case of VHH, the target protein band in P_{H36}-VHH constructs appeared at 6 h but was invisible in the supernatant of P_{A256}-VHH constructs at the same time (Fig. 4b). The fluorescence intensity from the

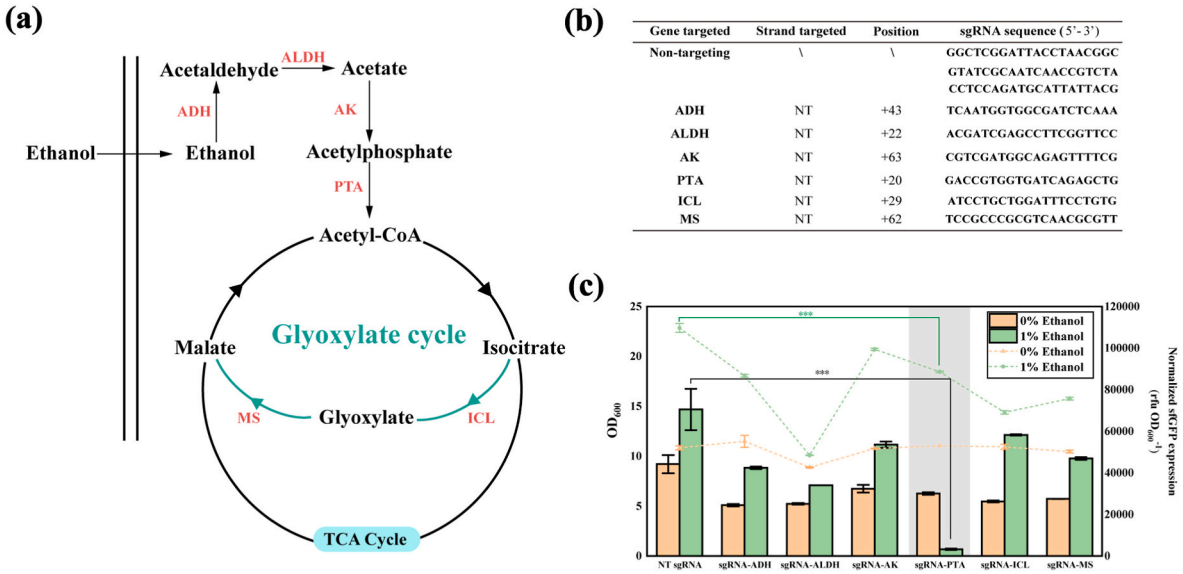

Gene targeted	Strand targeted	Position	sgRNA sequence (5'- 3')
Non-targeting	\	\	GGCTCGGATTACCTAACGGC GTATCGCAATCAACCGTCTA CCTCCAGATGCATTATTACG
ADH	NT	+43	TCAATGGTGGCGATCTCAAA
ALDH	NT	+22	ACGATCGAGCCTTCGGTTCC
AK	NT	+63	CGTCGATGGCAGAGTTTTCG
PTA	NT	+20	GACCGTGGTGATCAGAGCTG
ICL	NT	+29	ATCCTGCTGGATTTCCTGTG
MS	NT	+62	TCCGCCCGCGTCAACGCGTT

Fig. 3. Activity of P_{A256} in the EUT blocking strains. (a) Diagram of the EUT pathway in *C. glutamicum*. Six key enzymes involved in the EUT pathway are highlighted in red. Abbreviations: ADH alcohol dehydrogenase, ALDH acetaldehyde dehydrogenase, AK acetate kinase, PTA phosphotransacetylase, AK acetate kinase, PTA phosphotransacetylase. (b) Genes targeted by dCas9 and sgRNA sequences used. (c) Cell growth (dotted line) and P_{A256}-controlled sfGFP expression (column) in the EUT-blocking strains. The sfGFP expression was measured in 24-deep-well plates for 24 h (0% ethanol) and 36 h (1% ethanol). NT sgRNA group: three nontargeting sgRNAs; data are presented as the mean values ± s.d. of three clones with different sgRNAs (n = 3). For other groups, values and error bars reflect the mean ± s.d. of three biological replicates. ***$P < 0.001$, Student's two-tailed *t*-test.

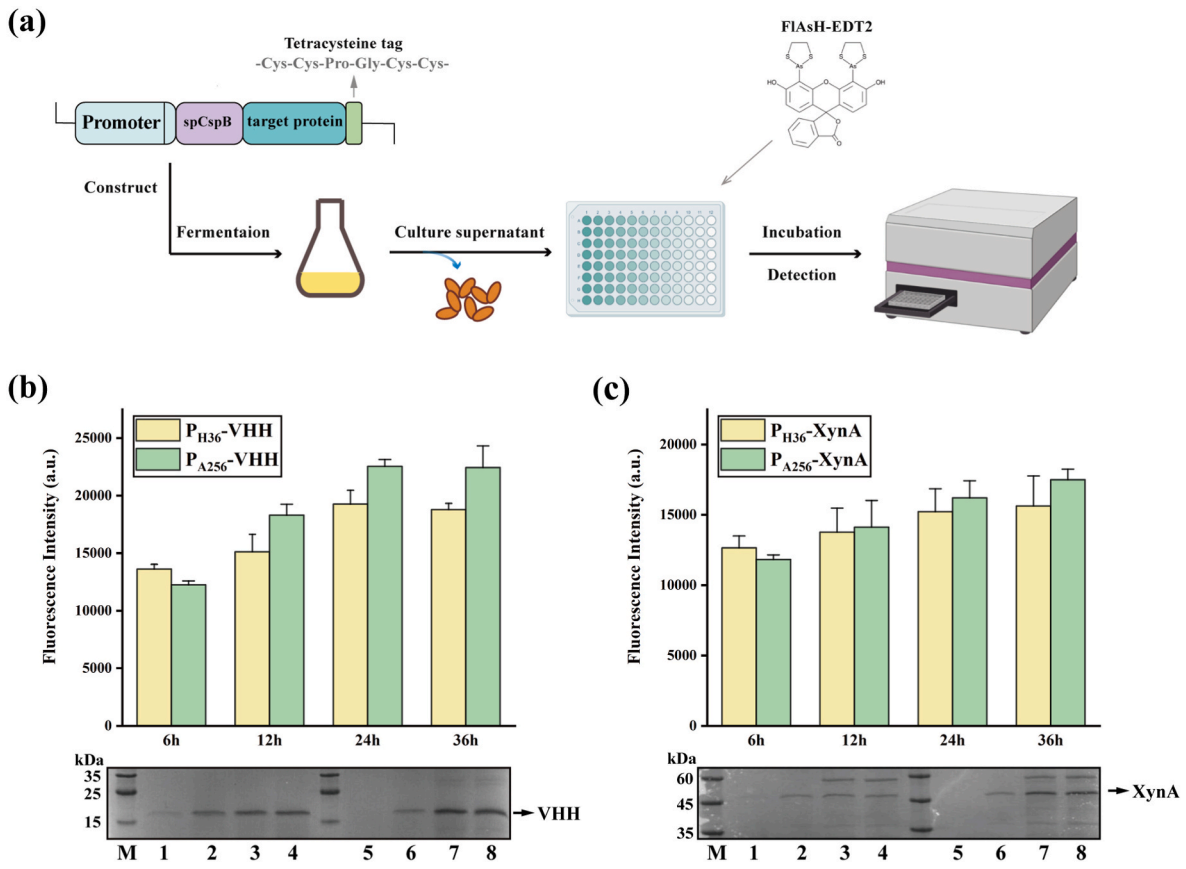

Fig. 4. Secretory protein expression controlled by P_{A256}. (a) Flowchart depicting the use of FLAsH-EDT_2 to detect secreted protein production. The tetracysteine tag was genetically fused to the C-terminus of the target proteins, and the culture supernatants of the corresponding constructs were diluted and mixed with FLAsH-EDT_2 in 96-well plates. After 1 h of incubation, the fluorescence generated corresponded to the content of labelled proteins and was measured by 485 nm excitation and 528 nm emission. (b)(c) The secreted protein (VHH, XynA) expression levels with P_{A256} and P_{H36} on 1% ethanol were characterized by fluorescence intensity (in different dilute forms, see methods). Protein production was conducted in shake flasks. Values and error bars reflect the mean ± s.d. of three biological replicates (n = 3). After centrifugation, culture supernatants were collected, and 15 μL denaturated samples were analyzed by SDS–PAGE. The VHH samples and XynA samples were analyzed by 15% (w/v) SDS–PAGE and 10% (w/v) SDS–PAGE, respectively. The arrow indicates the target protein. Lane M: Protein Marker; Lanes 1–4: H36 samples taken at 6, 12, 24 and 36 h; Lanes 5–8: A256 samples taken at 6, 12, 24 and 36 h.

FlAsH-tetracysteine reaction confirmed this result. This result indicated that the secretory protein expression controlled by P_{A256} was low during the early fermentation stage, which was compatible with the results of the intracellular sfGFP expression assay. The yield of VHH with P_{A256} surpassed that with P_{H36} after 12 h and remained higher until the end of fermentation. In XynA production, a lower preaccumulation and greater final yield expression pattern were also observed. (Fig. 4c). These results demonstrated that the A256 expression system provides a superior model for recombinant protein production in *C. glutamicum*.

3.6. Secretory production of NEO-2/15 using the A256 expression system

We also applied the A256 expression system to overexpress the new drug protein Neo-2/15 (Neo). As a "de novo design" protein, Neo mimics the effects of the central immune cytokines interleukin-2 and interleukin-15 [50]; to date, there has been no attempt to overexpress it in a secretory form. Initially, we attempted to secrete Neo using the Sec-type secretory signal peptide of CspB and Tat-type secretory signal peptide of CgR0949 [51], but only intracellular soluble NEO was detected in these two constructs (Fig. 5b). This indicated that NEO cannot be secreted through the Sec or Tat pathway only by the guidance of signal peptides. According to recent research, preprotein mature domains not only operate as passive passengers but also contain translocase targeting signals that are essential for secretion [52,53]. Therefore, we devised a novel approach to induce NEO secretory expression, i.e., fusion with a portion of the endogenous secretory protein CspB (Fig. 5a). For this purpose, NEO was genetically fused with the N-terminal 50 amino acid residues of CspB (namely CspB50, Text S4). As the results showed, despite the intracellular retention (target protein with the uncleaved signal peptide), the fused protein CspB50-NEO (C_{50}-NEO, ~19 kDa) could be detected in the culture supernatant (Fig. 5b). Then, the secretory production of C_{50}-NEO controlled by P_{A256} was evaluated by shaking-flask fermentation under the concentration of 1–2% ethanol (Fig. S8), and the greatest accumulation of C_{50}-NEO (281 mg/L) was achieved after 24 h cultivation with 1% ethanol added (Fig. 5c). To the best of our knowledge, this is the first report of recombinant protein secretion by fusion of the CspB protein in *C. glutamicum*.

4. Discussion

Due to its numerous ideal protein secretion properties, *C. glutamicum* has attracted attention in recent years as a potential cell factory for recombinant protein production. However, protein production with *C. glutamicum* is currently based on sugar-containing medium, which is incompatible with the biorefinery concept of converting renewable biomass to multiple high-value products [54]. Hence, the feasibility of using ethanol as a substrate for recombinant protein production is discussed here. To achieve efficient production of recombinant proteins on ethanol, we were inspired by the regulation of the MUT pathway and the *AOX1* promoter in *P. pastoris* and identified the promoter of isocitrate

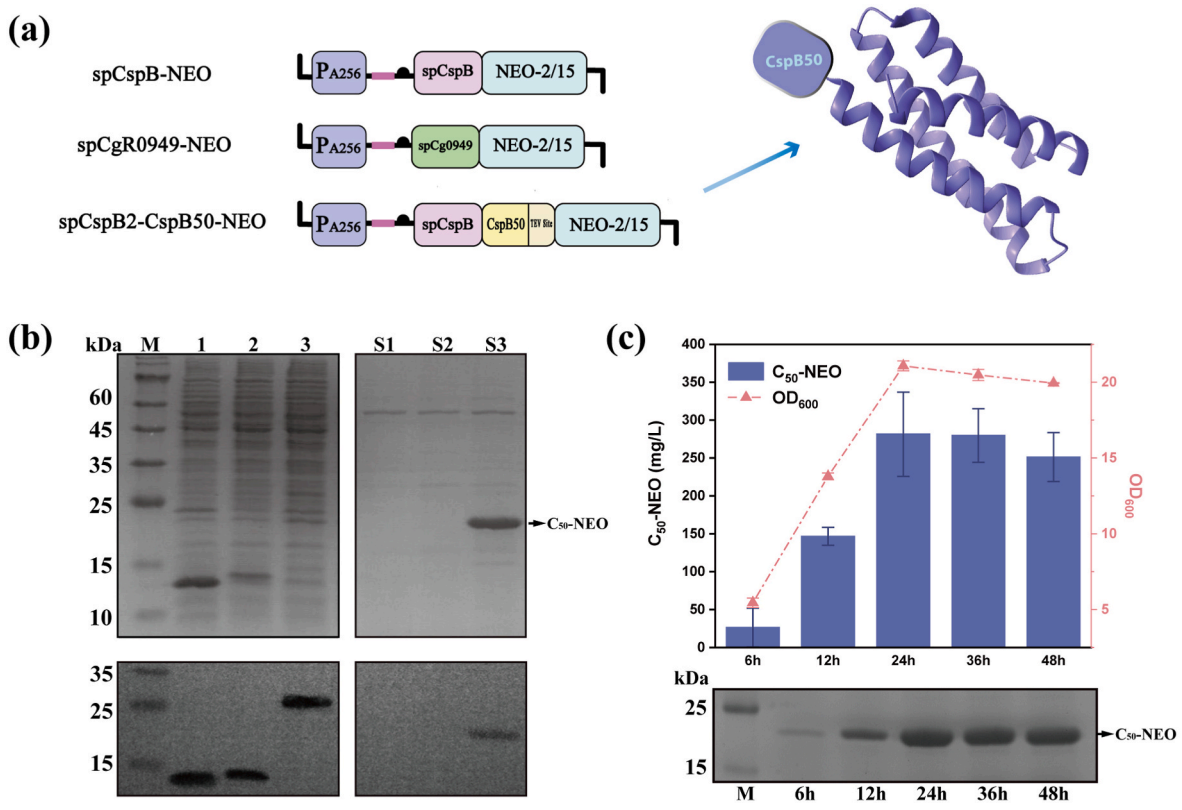

Fig. 5. Secretory production of NEO-2/15 using the A256 expression system. (a) Schematic diagram of plasmids constructed for Neo-2/15 expression. Different signal peptides were fused to the N-terminus of the target protein. spCgR0949, the secretory signal peptide of CgR0949. TEV site, the cleavage site of TEV protease. (b) SDS–PAGE and western blotting analysis of the intracellular soluble proteins and culture supernatants from the spCspB-NEO (Lanes 1&S1), spCgR0949-NEO (Lanes 2&S2) and spCspB-CspB50-NEO (Lanes 3&S3) constructs. Protein production was conducted in 24-deep-well plates. Samples were harvested after inoculation for 36 h, and the cellular proteins and culture supernatant proteins were analyzed by 15% (w/v) SDS–PAGE. The arrow indicates the target protein C_{50}-NEO. (c) Time profiles of the cell growth (linear graph) and NEO-2/15 concentration (bar graph) detected in the culture supernatant of spCspB-CspB50-NEO constructs on 1% ethanol. Values and error bars reflect the mean ± s.d. of three biological replicates (n = 3). Protein production was conducted in shake flasks. Lane M, Protein Marker; Lanes 1–4, samples taken at 6, 12, 24, 36 h, respectively.

lyase as the representative NOP triggering the EUT pathway in *C. glutamicum*. Although the native 5′UTR of P_{ICL} resulted in a very low translation initiation efficiency when expressing heterologous proteins, it could be repaired by bicistronic design or the introduction of a ribozyme-based insulator. Since self-cleavage ribozyme can remove the different upstream 5′ UTRs, transcriptional levels could be compared between promoter variants and positive control promoters. Based on this, transcriptional engineering was performed on the natural P_{ICL}, including engineering of TFBSs and UTR, and resulted in a particularly strong promoter, P_{A256}. Removal of the most distant RamA binding motif conferred a significantly increased transcriptional strength, despite the fact that RamA was identified as the activator of P_{ICL} [55], which indicated that the location of TFBS may correlate with its function. In addition, the nondeletionability of other TFBSs in P_{A256} was validated in our work; thus, duplication and rearrangement of existing TFBSs might be a possible strategy to further improve its transcriptional level in the future.

The protein expression controlled by P_{A256} went through three stages: 1) a very low expression level on plate and in the early growth period; 2) an increased expression level during the exponential growth phase with or without ethanol addition; and 3) a dramatically elevated expression level in the secondary growth driven by ethanol. Such an expression curve implies a lower burden on cells during proliferation, thus leading to a high density of production units. It has been reported that the specific activity of ICL significantly increased in RamB-deficient and GlxR-deficient strains irrespective of the substrate [39,40]; therefore, the low activity of P_{A256} in the early stage of growth may be the result of the regulation of these two transcription factors in response to preferential carbon sources. In the case of sfGFP expression, similar unit expression levels were obtained within the range of 1–2% ethanol addition, whereas higher amounts inhibited growth and protein expression. Tolerance to ethanol can be achieved in bacteria by altering the membrane lipid composition, such as increasing the length of fatty acid chains or the amount of nonpolar lipids [56]. Therefore, generating *C. glutamicum* strains with increased ethanol tolerance by genetic modification or adaptive evolution may be a viable option to further harness the benefits of the A256 expression system.

CRISPRi technology has been successfully applied to optimize the production of various metabolic intermediates and analyse gene function in *C. glutamicum* [57,58]. In this work, a single plasmid CRISPRi system was developed to downregulate the genes encoding enzymes involved in ethanol metabolism, and the performance of P_{A256} was investigated in these EUT blocking strains. Ethanol metabolism in *C. glutamicum* begins with a two-step oxidation to acetate, catalysed by ADH and an ALDH, and proceeds via acetate activation by AK and PTA and the glyoxylate cycle with ICL and MS as key enzymes. Among them, knocking down the PTA coding gene dramatically reduced P_{A256} activity under ethanol conditions. This suggests that the PTA-catalysed step, i.e., acetyl phosphatase activated to acetyl-CoA and entering the TCA cycle is a necessary prerequisite for the upregulation of P_{A256} on ethanol. Whereas P_{A256} is regulated by multiple global transcription factors and the effectors of which have yet to be identified, the exact regulatory mechanisms are a mystery that need more investigation.

By introducing the FlAsH-tetracysteine system, the performance of

different promoters in the secretory expression of various proteins can be easily compared. Thus, except for the intracellular fluorescent proteins, the high-efficiency production of two secretory proteins, VHH and XynA, also confirmed the advantages of the A256 expression system. Furthermore, the "de novo design" protein NEO-2/15 was successfully secreted into the medium by introducing a propeptide at the N-terminus, and a yield of 281 mg/L was obtained at the flask level using an A256 expression system. In conclusion, the ethanol-regulated A256 expression system showed significant potential in recombinant protein production, and we anticipated that it could be further developed through scale-up and fermentation process optimization.

Funding information

This work received funding from the National Natural Science Foundation of China (No. 21878124, 22078128, and 21938004), the Fundamental Research Funds for the Central Universities (No. JUSRP221032), the 111 Project (No. 111-2-06) and the national first-class discipline program of Light Industry Technology and Engineering (LITE2018-24).

Data availability

The datasets generated and analyzed during the current study are available from the corresponding author on reasonable request.

Author contributions

XY designed and performed most experiments. XL, XG and XL contributed to experimental planning and data analysis. All authors read and approved the final manuscript.

Ethical statement

This article does not contain any study with human participants or animals performed by any of the authors.

Declaration of competing interest

The authors declare that they have no conflict of interest.

Appendix A. Supplementary data

Supplementary data to this article can be found online at https://doi.org/10.1016/j.synbio.2022.03.004.

References

[1] Kesik-Brodacka M. Progress in biopharmaceutical development. Biotechnol Appl Biochem 2018;65:306–22. https://doi.org/10.1002/bab.1617.
[2] Walsh G. Biopharmaceutical benchmarks 2018. Nat Biotechnol 2018;36:1136–45. https://doi.org/10.1038/nbt.4305.
[3] Luis Corchero J, Gasser B, Resina D, Smith W, Parrilli E, Vazquez F, et al. Unconventional microbial systems for the cost-efficient production of high-quality protein therapeutics. Biotechnol Adv 2013;31:140–53. https://doi.org/10.1016/j.biotechadv.2012.09.001.
[4] Berlec A, Strukelj B. Current state and recent advances in biopharmaceutical production in Escherichia coli, yeasts and mammalian cells. J Ind Microbiol Biotechnol 2013;40:257–74. https://doi.org/10.1007/s10295-013-1235-0.
[5] Rosano GL, Morales ES, Ceccarelli EA. New tools for recombinant protein production in Escherichia coli: a 5-year update. Protein Sci 2019;28:1412–22. https://doi.org/10.1002/pro.3668.
[6] Freudl R. Beyond amino acids: use of the Corynebacterium glutamicum cell factory for the secretion of heterologous proteins. J Biotechnol 2017;258:101–9. https://doi.org/10.1016/j.jbiotec.2017.02.023.
[7] Anne J, Economou A, Bernaerts K. Protein secretion in gram-positive bacteria: from multiple pathways to biotechnology. In: Bagnoli F, Rappuoli R, editors. Curr top microbiol immunol, vol. 404. Berlin: Springer Verlag; 2017. p. 267–308. https://doi.org/10.1007/82_2016_49.
[8] Liu L, Yang H, Shin H-d, Li J, Du G, Chen J. Recent advances in recombinant protein expression by Corynebacterium, Brevibacterium, and Streptomyces: from transcription and translation regulation to secretion pathway selection. Appl Microbiol Biotechnol 2013;97:9597–608. https://doi.org/10.1007/s00253-013-5250-x.
[9] Harwood CR, Cranenburgh R. Bacillus protein secretion: an unfolding story. Trends Microbiol 2008;16:73–9. https://doi.org/10.1016/j.tim.2007.12.001.
[10] Wendisch VF, Jorge JMP, Perez-Garcia F, Sgobba E. Updates on industrial production of amino acids using Corynebacterium glutamicum. World J Microbiol Biotechnol 2016;32(6):105. https://doi.org/10.1007/s11274-016-2060-1.
[11] Lee MJ, Kim P. Recombinant protein expression system in Corynebacterium glutamicum and its application. Front Microbiol 2018;9:2523. https://doi.org/10.3389/fmicb.2018.02523.
[12] Xu D, Tan Y, Shi F, Wang X. An improved shuttle vector constructed for metabolic engineering research in Corynebacterium glutamicum. Plasmid 2010;64:85–91. https://doi.org/10.1016/j.plasmid.2010.05.004.
[13] Yim SS, An SJ, Kang M, Lee J, Jeong KJ. Isolation of fully synthetic promoters for high-level gene expression in Corynebacterium glutamicum. Biotechnol Bioeng 2013;110:2959–69. https://doi.org/10.1002/bit.24954.
[14] Li N, Zeng W, Xu S, Zhou J. Obtaining a series of native gradient promoter-5 '-UTR sequences in Corynebacterium glutamicum ATCC 13032. Microb Cell Factories 2020;19:120. https://doi.org/10.1186/s12934-020-01376-3.
[15] Okibe N, Suzuki N, Inui M, Yukawa H. Isolation, evaluation and use of two strong, carbon source-inducible promoters from Corynebacterium glutamicum. Lett Appl Microbiol 2010;50:173–80. https://doi.org/10.1111/j.1472-765X.2009.02776.x.
[16] Ata O, Prielhofer R, Gasser B, Mattanovich D, Calik P. Transcriptional engineering of the glyceraldehyde-3-phosphate dehydrogenase promoter for improved heterologous protein production in Pichia pastoris. Biotechnol Bioeng 2017;114:2319–27. https://doi.org/10.1002/bit.26363.
[17] Ergun BG, Gasser B, Mattanovich D, Calik P. Engineering of alcohol dehydrogenase 2 hybrid-promoter architectures in Pichia pastoris to enhance recombinant protein expression on ethanol. Biotechnol Bioeng 2019;116:2674–86. https://doi.org/10.1002/bit.27095.
[18] Hartner FS, Ruth C, Langenegger D, Johnson SN, Hyka P, Lin-Cereghino GP, et al. Promoter library designed for fine-tuned gene expression in Pichia pastoris. Nucleic Acids Res 2008;36:e76. https://doi.org/10.1093/nar/gkn369.
[19] Arndt A, Auchter M, Ishige T, Wendisch VF, Eikmanns BJ. Ethanol catabolism in Corynebacterium glutamicum. J Mol Microbiol Biotechnol 2008;15:222–33. https://doi.org/10.1159/000107370.
[20] Patek M, Holatko J, Busche T, Kalinowski J, Nesvera J. Corynebacterium glutamicum promoters: a practical approach. Microb Biotechnol 2013;6:103–17. https://doi.org/10.1111/1751-7915.12019.
[21] Ruan Y, Zhu L, Li Q. Improving the electro-transformation efficiency of Corynebacterium glutamicum by weakening its cell wall and increasing the cytoplasmic membrane fluidity. Biotechnol Lett 2015;37:2445–52. https://doi.org/10.1007/s10529-015-1934-x.
[22] Zhao Z, Liu X, Zhang W, Yang Y, Dai X, Bai Z. Construction of genetic parts from the Corynebacterium glutamicum genome with high expression activities. Biotechnol Lett 2016;38:2119–26. https://doi.org/10.1007/s10529-016-2196-y.
[23] Gibson DG, Young L, Chuang R-Y, Venter JC, Hutchison III CA, Smith HO. Enzymatic assembly of DNA molecules up to several hundred kilobases. Nat Methods 2009;6. https://doi.org/10.1038/nmeth.1318. 343-U41.
[24] Engler C, Kandzia R, Marillonnet S. A one pot, one step, precision cloning method with high throughput capability. PLoS One 2008;3:e3647. https://doi.org/10.1371/journal.pone.0003647.
[25] Jiang H, Wong WH. SeqMap: mapping massive amount of oligonucleotides to the genome. Bioinformatics 2008;24:2395–6. https://doi.org/10.1093/bioinformatics/btn429.
[26] Wang X, Peng F, Dong G, Sun Y, Dai X, Yang Y, et al. Identification and validation of appropriate reference genes for qRT-PCR analysis in Corynebacterium glutamicum. FEMS Microbiol Lett 2018;365. https://doi.org/10.1093/femsle/fny030.
[27] Liu X, Yang Y, Zhang W, Sun Y, Peng F, Jeffrey L, et al. Expression of recombinant protein using Corynebacterium Glutamicum: progress, challenges and applications. Crit Rev Biotechnol 2016;36:652–64. https://doi.org/10.3109/07388551.2015.1004519.
[28] Reinscheid DJ, Eikmanns BJ, Sahm H. Characterization of the isocitrate lyase gene from corynebacterium-glutamicum and biochemical-analysis of the enzyme. J Bacteriol 1994;176:3474–83. https://doi.org/10.1128/jb.176.12.3474-3483.1994.
[29] Reinscheid DJ, Eikmanns BJ, Sahm H. Malate synthase from Corynebacterium glutamicum: sequence analysis of the gene and biochemical characterization of the enzyme. Microbiology-Sgm 1994;140:3099–108. https://doi.org/10.1099/13500872-140-11-3099.
[30] Maeda T, Wachi M. 3 ' untranslated region-dependent degradation of the aceA mRNA, encoding the glyoxylate cycle enzyme isocitrate lyase, by RNase E/G in Corynebacterium glutamicum. Appl Environ Microbiol 2012;78:8753–61. https://doi.org/10.1128/aem.02304-12.
[31] Cetnar DP, Salis HM. Systematic quantification of sequence and structural determinants controlling mRNA stability in bacterial operons. ACS Synth Biol 2021;10:318–32. https://doi.org/10.1021/acssynbio.0c00471.
[32] Sun M, Gao X, Zhao Z, Li A, Wang Y, Yang Y, et al. Enhanced production of recombinant proteins in Corynebacterium glutamicum by constructing a bicistronic gene expression system. Microb Cell Factories 2020;19:113. https://doi.org/10.1186/s12934-020-01370-9.
[33] Liu X, Zhao Z, Dong G, Li Y, Peng F, Liu C, et al. Identification, repair and characterization of a benzyl alcohol-inducible promoter for recombinant proteins

overexpression in Corynebacterium glutamicum. Enzym Microb Technol 2020;141. https://doi.org/10.1016/j.enzmictec.2020.109651.
[34] Liu X, Zhao Z, Zhang W, Sun Y, Yang Y, Bai Z. Bicistronic expression strategy for high-level expression of recombinant proteins in Corynebacterium glutamicum. Eng Life Sci 2017;17:1118–25. https://doi.org/10.1002/elsc.201700087.
[35] Mutalik VK, Guimaraes JC, Cambray G, Lam C, Christoffersen MJ, Quynh-Anh M, et al. Precise and reliable gene expression via standard transcription and translation initiation elements. Nat Methods 2013;10:354. https://doi.org/10.1038/nmeth.2404.
[36] Gerstmeir R, Wendisch VF, Schnicke S, Ruan H, Farwick M, Reinscheid D, et al. Acetate metabolism and its regulation in Corynebacterium glutamicum. J Biotechnol 2003;104:99–122. https://doi.org/10.1016/s0168-1656(03)00167-6.
[37] Toyoda K, Inui M. Regulons of global transcription factors in Corynebacterium glutamicum. Appl Microbiol Biotechnol 2016;100:45–60. https://doi.org/10.1007/s00253-015-7074-3.
[38] Cramer A, Gerstmeir R, Schaffer S, Bott M, Eikmanns BJ. Identification of RamA, a novel LuxR-type transcriptional regulator of genes involved in acetate metabolism of Corynebacterium glutamicum. J Bacteriol 2006;188:2554–67. https://doi.org/10.1128/jb.188.7.2554-2567.2006.
[39] Gerstmeir R, Cramer A, Dangel P, Schaffer S, Eikmanns BJ. RamB, a novel transcriptional regulator of genes involved in acetate metabolism of Corynebacterium glutamicum. J Bacteriol 2004;186:2798–809. https://doi.org/10.1128/jb.186.9.2798-2809.2004.
[40] Park S-Y, Moon M-W, Subhadra B, Lee J-K. Functional characterization of the glxR deletion mutant of Corynebacterium glutamicum ATCC 13032: involvement of GlxR in acetate metabolism and carbon catabolite repression. FEMS Microbiol Lett 2010;304:107–15. https://doi.org/10.1111/j.1574-6968.2009.01884.x.
[41] Lou C, Stanton B, Chen Y-J, Munsky B, Voigt CA. Ribozyme-based insulator parts buffer synthetic circuits from genetic context. Nat Biotechnol 2012;30:1137. https://doi.org/10.1038/nbt.2401.
[42] Hsu LM, Cobb IM, Ozmore JR, Khoo M, Nahm G, Xia L, et al. Initial transcribed sequence mutations specifically affect promoter escape properties. Biochemistry 2006;45:8841–54. https://doi.org/10.1021/bi060247u.
[43] Haenssler E, Mueller T, Palumbo K, Patek M, Brocker M, Kraemer R, et al. A game with many players: control of gdh transcription in Corynebacterium glutamicum. J Biotechnol 2009;142:114–22. https://doi.org/10.1016/j.jbiotec.2009.04.007.
[44] Larson MH, Gilbert LA, Wang X, Lim WA, Weissman JS, Qi LS. CRISPR interference (CRISPRi) for sequence-specific control of gene expression. Nat Protoc 2013;8:2180–96. https://doi.org/10.1038/nprot.2013.132.
[45] Yim SS, Choi JW, Lee RJ, Lee YJ, Lee SH, Kim SY, et al. Development of a new platform for secretory production of recombinant proteins in Corynebacterium glutamicum. Biotechnol Bioeng 2016;113:163–72. https://doi.org/10.1002/bit.25692.
[46] Martin BR, Giepmans BNG, Adams SR, Tsien RY. Mammalian cell-based optimization of the biarsenical-binding tetracysteine motif for improved fluorescence and affinity. Nat Biotechnol 2005;23:1308–14. https://doi.org/10.1038/nbt1136.
[47] Haitjema CH, Boock JT, Natarajan A, Dominguez MA, Gardner JG, Keating DH, et al. Universal genetic assay for engineering extracellular protein expression. ACS Synth Biol 2014;3:74–82. https://doi.org/10.1021/sb400142b.
[48] Adams SR, Campbell RE, Gross LA, Martin BR, Walkup GK, Yao Y, et al. New biarsenical Ligands and tetracysteine motifs for protein labeling in vitro and in vivo: synthesis and biological applications. J Am Chem Soc 2002;124:6063–76. https://doi.org/10.1021/ja017687n.
[49] Zhang W, Yang Y, Liu X, Liu C, Bai Z. Development of a secretory expression system with high compatibility between expression elements and an optimized host for endoxylanase production in Corynebacterium glutamicum. Microb Cell Factories 2019;18:72. https://doi.org/10.1186/s12934-019-1116-y.
[50] Silva D-A, Yu S, Ulge UY, Spangler JB, Jude KM, Labao-Almeida C, et al. De novo design of potent and selective mimics of IL-2 and IL-15. Nature 2019;565:186. https://doi.org/10.1038/s41586-018-0830-7.
[51] Teramoto H, Watanabe K, Suzuki N, Inui M, Yukawa H. High yield secretion of heterologous proteins in Corynebacterium glutamicum using its own Tat-type signal sequence. Appl Microbiol Biotechnol 2011;91:677–87. https://doi.org/10.1007/s00253-011-3281-8.
[52] Chatzi KE, Sardis MF, Tsirigotaki A, Koukaki M, Sostaric N, Konijnenberg A, et al. Preprotein mature domains contain translocase targeting signals that are essential for secretion. J Cell Biol 2017;216:1357–69. https://doi.org/10.1083/jcb.201609022.
[53] Sardis MF, Tsirigotaki A, Chatzi KE, Portaliou AG, Gouridis G, Karamanou S, et al. Preprotein conformational dynamics drive bivalent translocase docking and secretion. Structure 2017;25:1056. https://doi.org/10.1016/j.str.2017.05.012.
[54] Ragauskas AJ, Williams CK, Davison BH, Britovsek G, Cairney J, Eckert CA, et al. The path forward for biofuels and biomaterials. Science 2006;311:484–9. https://doi.org/10.1126/science.1114736.
[55] Shah A, Blombach B, Gauttam R, Eikmanns BJ. The RamA regulon: complex regulatory interactions in relation to central metabolism in Corynebacterium glutamicum. Appl Microbiol Biotechnol 2018;102:5901–10. https://doi.org/10.1007/s00253-018-9085-3.
[56] Ingram LO. Ethanol tolerance in bacteria. Crit Rev Biotechnol 1990;9:305–19.
[57] Yoon J, Woo HM. CRISPR interference-mediated metabolic engineering of Corynebacterium glutamicum for homo-butyrate production. Biotechnol Bioeng 2018;115:2067–74. https://doi.org/10.1002/bit.26720.
[58] Lee SS, Shin H, Jo S, Lee S-M, Um Y, Woo HM. Rapid identification of unknown carboxyl esterase activity in Corynebacterium glutamicum using RNA-guided CRISPR interference. Enzym Microb Technol 2018;114:63–8. https://doi.org/10.1016/j.enzmictec.2018.04.004.